

ORIGINAL ARTICLE

Construction of amperometric biosensor modified with conducting polymer/carbon dots for the analysis of catechol

Mustafa Yasa¹  | Aybuke Deniz² | Mehrdad Forough²  | Erol Yildirim^{1,2}  |
Ozgul Persil Cetinkol²  | Yasemin Arslan Udum³  | Levent Toppare^{1,2,4,5} 

¹Department of Polymer Science and Technology, Middle East Technical University, Ankara, Turkey

²Department of Chemistry, Middle East Technical University, Ankara, Turkey

³Technical Sciences Vocational High School, Gazi University, Ankara, Turkey

⁴Department of Biotechnology, Middle East Technical University, Ankara, Turkey

⁵The Center for Solar Energy and Applications, Middle East Technical University, Ankara, Turkey

Correspondence

Yasemin Arslan Udum, Technical Sciences Vocational High School, Gazi University, 06374, Ankara, Turkey
Email: y.udum@gazi.edu.tr

Abstract

Phenolic compounds used in food industries and pesticide industry, are environmentally toxic and pollute the rivers and ground water. For that reason, detection of phenolic compounds such as catechol by using simple, efficient and cost-effective devices have been becoming increasingly popular. In this study, a suitable and a novel matrix was composed using a novel conjugated polymer, namely poly[1-(5-(4,8-bis(5-(2-ethylhexyl)thiophen-2-yl)benzo[1,2-b:4,5-b']dithiophen-2-yl)furan-2-yl)-5-(2-ethylhexyl)-3-(furan-2-yl)-4H thieno[3,4-c]pyrrole-4,6(5H)-dione] (PFTBDT) and carbon dots (CDs) to detect catechol. PFTBDT and CDs were synthesized and the optoelectronic properties of PFTBDT were investigated via electrochemical and spectroelectrochemical studies. Laccase enzyme was immobilized onto the constructed film matrix on the graphite electrode. The proposed biosensor was found to have a low detection limit (1.23 μM) and a high sensitivity (737.44 $\mu\text{A}/\text{mM}\cdot\text{cm}^{-2}$) with a linear range of 1.25–175 μM . Finally, the applicability of the proposed enzymatic biosensor was evaluated in a tap water sample and a satisfactory recovery (96–104%) was obtained for catechol determination.

KEYWORDS

carbon dots, catechol, conjugated polymer, enzyme-based biosensor, phenolic compounds

1 | INTRODUCTION

Identification and quantification of phenolic compounds have received exceptional interest from the scientific community owing to their high toxicity in nature, water resources and human health. Between the phenolic compounds, Catechol (1, 2- hydroxybenzene or 1, 2-benzenediol), is found in many everyday products, such as cosmetics, pesticides, pharmaceuticals and food additives.¹ It has been classified as a periodic toxic pollutant. The US Environmental Protection Agency (US EPA) and the European Commission (EC) have created a list and special attention has been devoted to catechol because of its low degradation rate and high toxicity.² Different

analytical methods have been utilized for the detection of catechol, such as fluorescence,³ high performance liquid chromatography,⁴ and chemiluminescence.⁵ However, most of these techniques are not considered as practical and up to expected standards mainly due to their low sensitivity, high cost, extensive time and sample handling/preparation requirements. Enzyme-based electrochemical biosensors, that overcome the aforementioned drawbacks, can be one alternative to the current techniques. Enzyme-based electrochemical biosensors are generally robust and facile sensing systems with relatively low overall cost.⁶ Most importantly, enzyme-based biosensors are highly selective and sensitive due to their specific high affinity toward their substrate.⁷ Detection of

catechol or other phenolic compounds can be achieved by using tyrosinase, laccase or peroxidase enzyme-based biosensors.

Laccases (benzenediol-oxygen oxidoreductase, E.C. 1.10.3.2) are copper containing enzymes found in higher plants, fungi, bacteria, and insects. They reduce oxygen to water during oxidation of phenolic compounds in four electron transfer steps without the formation of hydrogen peroxide.⁸ Laccases have found use in various industries, such as bioremediation, paper and pulp, pharmaceutical, textile and food industries, besides being used in biosensors.⁹ One downside of the laccase biosensors is their stability. To provide suitable matrix for enzyme immobilization and to enhance stability, conducting polymers (CPs) have been used in analytical systems due to their special optoelectronic properties.^{10–12}

The use of conducting polymer films to improve analytical performance appears to be a strong candidate for the development of biosensors. CPs permit easy localization of biomolecules on transducer surface and enhance the charge transfer between the active site of the enzyme and the electrode. Accordingly, they enhance the stability, sensitivity and the response time of the biosensors by providing a suitable matrix for enzyme immobilization.¹³ Thieno[3,4-c]pyrrole-4,6-dione-TPD has been used as an acceptor moiety in various conjugated polymers utilized for organic solar cells. TPD has a simple, symmetric, fused, planar and compact structure leading to electron delocalization through the backbone of the polymer.^{14–17} Due to geometric strain, it exhibits decreased steric repulsion between the neighboring units. Additionally, the interactions between the sulfur and oxygen atoms lead to backbone planarity. These features make TPD-based polymers to have relatively lower band gaps and closer π - π interactions, consequently facilitating the improved charge transport.¹⁸ Its strong electron-withdrawing effect leads to lower highest occupied molecular orbital/Lowest unoccupied molecular orbital (HOMO/LUMO) energy levels and makes TPD a good accomplice in both intermolecular and intramolecular interactions.^{19,20} Besides, TPD is able to stabilize itself by gaining a quinoidal thiophene-maleimide structure during excitation resulting in lower band gap energy.²¹ TPD moiety can also be modified easily through the donor benzodithiophene-BDT, mostly to improve polymer's solubility via the introduction of alkyl chains. Thus, due to its remarkable features, TPD moiety has been widely incorporated into conjugated polymers via Stille polycondensation reaction.

One of the most critical steps in the fabrication of enzyme-based biosensors is enzyme immobilization. In this step, it is important to attach the recognizing element effectively. Otherwise, enzyme may leak from the

electrode surface during analysis hence reducing the signal and sensitivity of the biosensor. Over the last 20 years, the use of nanomaterials in the construction of biosensing devices offer unique characteristics that give sensitive detection of catechol, such as carbon nanomaterials, metal and metal alloy nanoparticles, and metal oxides. The small dimensions of nanomaterials contribute greatly in obtaining a surface that has an excellent adsorption property. Since nanomaterials have high chemical stability and high surface to volume ratio, they provide biocompatible matrices for biosensor applications.²² Carbon dots (CDs) are a relatively new class of zero-dimensional (0-D) carbon nanomaterials.²³ Even though CDs have become powerful tools in chemo- and bio-sensing applications, they have not been explored widely in electrochemical biosensor applications.^{24–26} Their excellent properties like low cytotoxicity, simple synthesis, remarkable conductivity and tunable luminescence activity enable CDs to be useful nanomaterials in electrochemical biosensor applications. Besides, their large surface area, ease of modification and excellent biocompatibility allow them to increase the amperometric response significantly.²⁷

Motivated by the abovementioned shortcomings of current techniques in catechol detection, we constructed a new biosensor using a thienopyrrole based conjugated polymer (PFTBDT) and CDs on graphite electrode. While carbon dots increase electrochemical signal of biosensor, the polymer enhances the stability and reduces the response time in the constructed biosensor for catechol detection. The use of an enzyme-based electrochemical biosensor is a simple, sensitive and low-cost alternative to other analytical methods for catechol determination. The developed sensor was found to have a wider linear dynamic range (LDR), lower limit of detection (LOD) and higher sensitivity compared to other catechol biosensors based on laccase. The results obtained in here show that the biosensor is most sensitive and has a potential use for catechol detection.

2 | EXPERIMENTAL

2.1 | Materials and methods

Thiophene-3,4-dicarboxylic acid, 2-(tributylstannyl) furan, laccase (Lac, EC 1.10.3.2 from *T. versicolor*, 21.8 Unit/mg), glucose, ethanol, glutaraldehyde (50% wt in H₂O), catechol (as a substrate), and all reagents were purchased from Sigma-Aldrich (Europe) and used without further purification. 4,8-bis[5-(2-ethylhexyl) thiophen-2-yl]-2,6-bis(trimethylstannyl)benzo[1,2-b:4,5-b'] dithiophene was purchased from Solarmer Materials Inc. (Beijing, China).

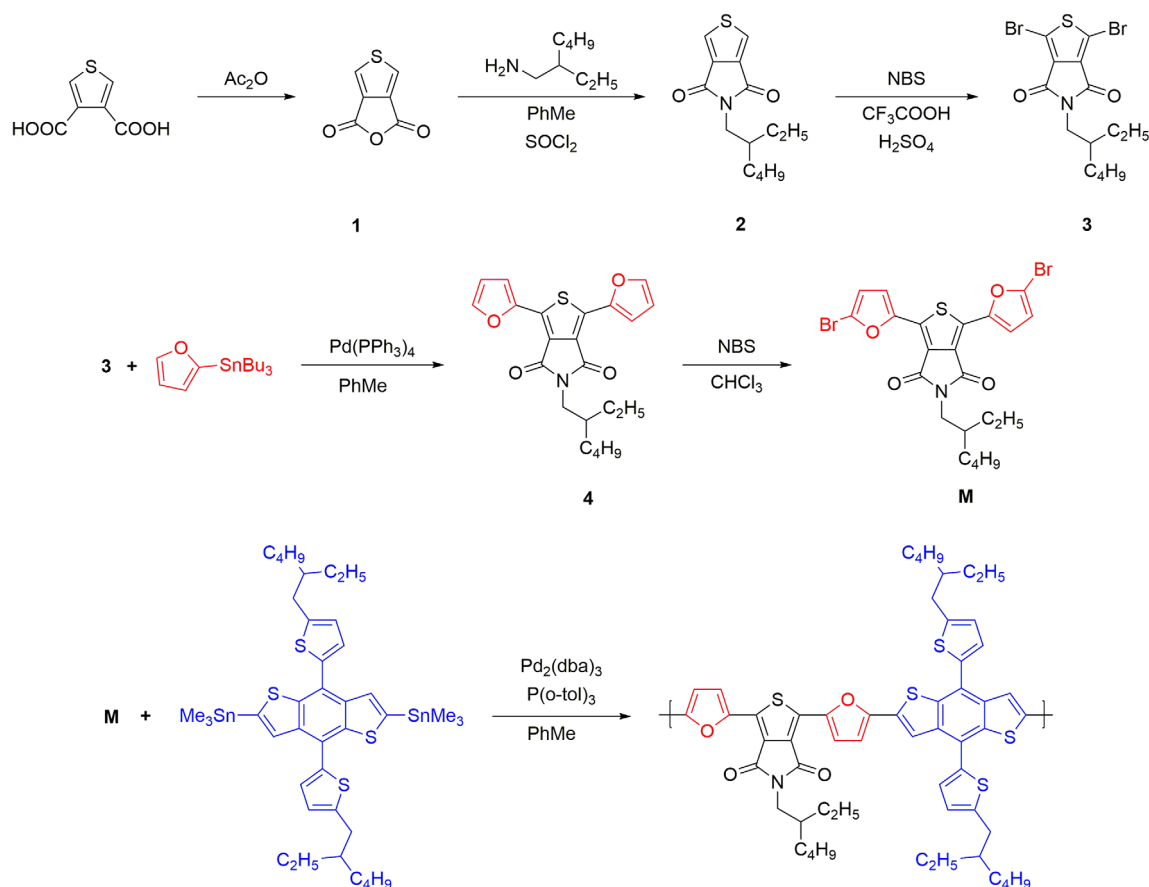
NMR spectra were recorded on a Bruker Spectrospin Avance DPX-400 Spectrometer. Number-average (M_n) and weight-average (M_w) molecular weights of the polymer were obtained by size exclusion chromatography via a Shimadzu LC-20AT GPC in chloroform at 40°C. All electrochemical measurements were performed with a three-electrode system. A platinum (Pt) wire and a silver (Ag) wire were used as the counter and the reference electrodes, respectively, while indium tin oxide (ITO) coated glass substrate was used as the working electrode. All potentials are referred to the pseudo-reference Ag electrode (+ 0.3 V vs Fc/Fc⁺). Spectroelectrochemical measurements were conducted with Varian Cary 5000 UV-Vis spectrophotometer and cyclic voltammograms (CV) of the polymer films were recorded using a GAMRY Reference 600 potentiostat. In chronoamperometric measurements, a modified graphite electrode (RW001 type, 0.07 cm²) was used as the working electrode. Amperometric studies were performed with PalmSens potentiostat. Crystallinity of carbon dots was investigated via X-ray diffraction (Rigaku Ultima-IV). Surface characterizations of the modified electrodes were performed by scanning electron microscopy (SEM) using a JEOL JSM-6400.

2.2 | Syntheses of monomers and CDs

CDs were synthesized according to a previously reported hydrothermal method with a minor modification.²⁸ The details are given in Supporting Information (Figure S1). Desired molecules were synthesized according to reported procedures (Scheme 1).²⁹ PFTBDT was synthesized via Stille polycondensation reaction.

2.3 | Preparation of modified electrode for biosensor application

To prepare the modified electrodes, bare graphite electrodes were first polished with emery paper and then thoroughly washed with distilled water. First, 0.5 mg ml⁻¹ CDs solution was prepared and dispersed in N, N-dimethylformamide (DMF). Five microliters of the prepared solution was drop cast on the cleaned graphite electrode and allowed to air-dry for 1 h at room temperature. Afterwards, 10.0 μl of the PFTBDT solution (1.25 mg per 1.0 ml of chloroform) was coated on CDs-modified electrode. CDs/PFTBDT-modified electrodes were allowed to air-dry followed by a distilled water wash



SCHEME 1 Synthetic pathway for the monomer and the polymer [Color figure can be viewed at wileyonlinelibrary.com]

before enzyme immobilization. Ten microliters of laccase enzyme (10.9 U) in phosphate buffer solution (pH 7.0, 50 mM) and glutaraldehyde solution (1% in H₂O) as a cross linking agent were added onto the modified electrodes and CDs/PFTBDT/Lac electrodes were allowed to dry at room temperature for 2 h. Finally, the electrodes were washed with distilled water to remove any unbound enzyme molecules, before used.

2.4 | Amperometric measurements for detection of catechol

Amperometric measurements were carried out at ambient temperature in a sample holder that contains 10 ml sodium acetate buffer (50 mM, pH 5.5). After the working electrode reached to equilibrium, catechol solution (as the substrate) was added to buffer solution and the current of the working electrode was monitored until a new equilibrium was established. The difference between two steady state current values (μA) were recorded as the biosensor's response. After each measurement, the electrodes were washed with distilled water and reaction medium was refreshed. Amperometric measurements were performed at -0.3 V which represents the biological activity of the enzyme. Additional experimental details and full characterization data including the NMR spectra are given in Supporting Information.

2.5 | Computational methods

Density functional theory (DFT) calculations were performed by using the B3LYP/6-311G*hybrid functional^{30–32} and basis set, using 10^{-8} RMS density matrix convergence and 10^{-6} energy change criteria in Gaussian09 (Revision A.02).³³ Successful results were achieved previously at this level of calculations for donor-acceptor studies in the literature.^{34,35} Results are validated by novel and promising TPSSh functional.³⁶ HOMO, LUMO, electrostatic potential surfaces (ESP), counterpoise corrected interaction energy of PFTBDT with catechol and effect of catechol on the electronic structure such as charge transfer were calculated for the geometry optimized structures of tetramer model oligomers with methyl side chains. Vertical excitation energy of the first singlet excited state $S_0 \rightarrow S_1$ were calculated by TDDFT calculations in acetonitrile solvent effect. Vertical ionization potential and vertical electron affinity were calculated by the energy difference between the neutral tetramer and cation state of the optimized ground state geometry. Reorganization energies (λ_{reorg}) for the holes were estimated based on the formulation by Bredas et al.³⁷ Periodic cells were minimized by

molecular mechanics methods to understand packing structure of polymer by adopting polymer consistent force field³⁸ for 10,000 steps with 12 Å cutoff atomic distance for vdW interactions and Ewald summation for electrostatic interactions.

3 | RESULTS

3.1 | Electrochemical and optical properties of PFTBDT

CV technique was used to investigate the electrochemical behavior of PFTBDT polymer. Using the CV technique, redox behavior and doping characteristics of the polymer were examined. Also, HOMO energy level was calculated from cyclic voltammogram of the polymer by spraying the polymer solution (6.0 mg of PFTBDT in 1.0 ml of chloroform) onto the glass substrate coated with indium tin oxide (ITO).

Three electrode system was used in CV experiments, constructed using a silver wire as the pseudo-reference, platinum wire as the counter and the prepared ITO as the working electrode, respectively. The CV studies were performed at a scan rate of 100 mV/s, under a potential range between 0 and 1.7 V in 0.1 M TBAPF₆/ACN electrolytic medium. The polymer is p-dopable. It was doped at 1.47 V and de-doped at 0.98 V. The HOMO energy was determined as -5.67 eV via onset value of the corresponding oxidation potential using Equation 1 where the normal hydrogen electrode was taken as -4.75 eV against vacuum. The corresponding oxidation potential was determined from the interception of the tangent line drawn from the peak and the baseline in the related cyclic voltammograms (Figure 1(A)).

$$\text{HOMO} = -(4.75 + E_{\text{ox,onset}}) \text{ (eV)} \quad (1)$$

The LUMO energy was determined from the difference between the optical band gap at neutral state and value of HOMO energy level. The LUMO energy level was found as -4.15 eV. Summary of the electrochemical parameters for the polymer is shown in Figure 1(B).

Spectroelectrochemical studies were performed to complement the electrochemical investigation of PFTBDT thin films. The experimental procedure for the preparation of the thin film was almost the same with electrochemical studies. Here, stepwise potential with appropriate increments was applied to the thin film. The response of the film to the applied potential was detected using UV-Vis Spectrophotometer (Figure 2(A)). The maximum absorption peak of polymer-coated thin film

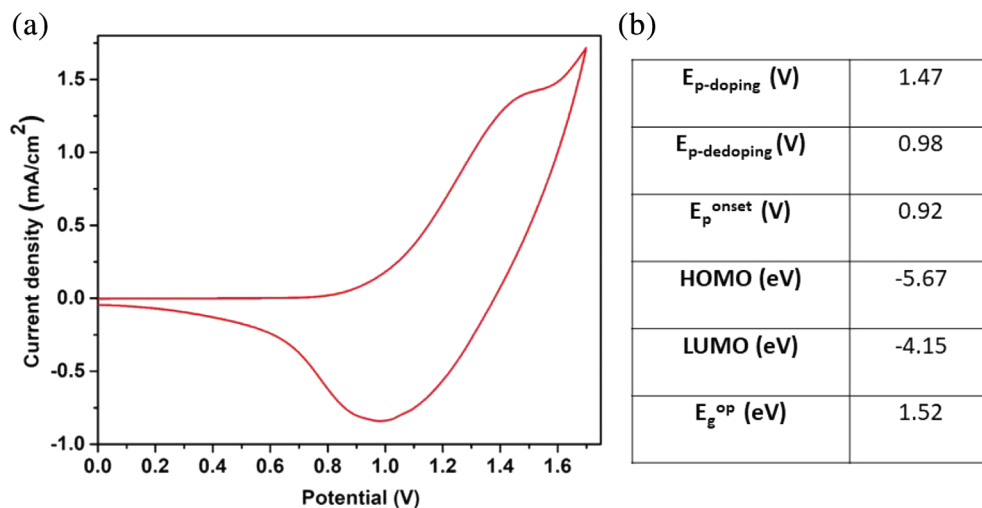


FIGURE 1 (A) Cyclic voltammogram of thienopyrrole based conjugated polymer (PFTBDT) in 0.1 M TBAPF₆/ACN solution and (B) electrochemical parameters of PFTBDT [Color figure can be viewed at wileyonlinelibrary.com]

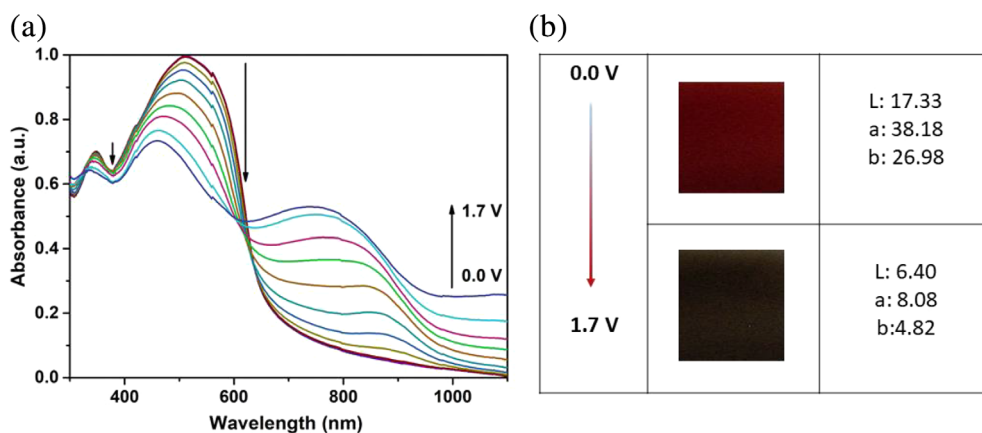


FIGURE 2 (A) Electronic absorption spectra and (B) Colorimetric measurements of thienopyrrole based conjugated polymer (PFTBDT) thin film in 0.1 M TBAPF₆/ACN solution [Color figure can be viewed at wileyonlinelibrary.com]

in the neutral state was observed at 515 nm. The intensity of this peak was decreased with increasing applied potential. Conversely, a polaron band arose with the increasing applied voltage. The polymer film was reddish green at 1.7 V, while it was dark red in neutral state. Optical band gap of the polymer was calculated as 1.52 eV using the onset value which was obtained from the intercept of the baseline and the tangent from the maximum absorption peak at neutral state.

Colorimetric investigations of the polymer film were also performed to determine L, a and b values defined by CIE (Commission Internationale de l'Eclairage) where L stands for luminescence, a stands for red/green and b stands for yellow/blue coordinates, respectively. The observed color change along with the corresponding L, a and b values are depicted in Figure 2(B).

PFTBDT polymer films are known to oscillate between their neutral and p-doped states. Hence, the kinetic studies were performed to obtain the optical contrast, the percent change in transmittance, and switching times of the

polymer using UV-Vis Spectrophotometer. Measurements were performed via the application of varying square-wave potentials between 0 and 1.7 V within 5 s periods. Percent optical contrasts between neutral and p-doped states were measured as 9 and 30% at 515 and 755 nm, respectively. The switching times were determined as 2.5 and 0.9 s at 515 and 755 nm, respectively from the time duration between the two applied voltages at a 95% contrast. Percent transmittance changes of the polymer film at 515 and 755 nm are depicted in Figure 3(A) and the obtained kinetic parameters are given in Figure 3(B).

3.2 | Electrochemical and surface characterization of electrodes and carbon dot nanoparticles

Characterizations of the effective surface area of the modified electrodes were investigated via CV. Voltammograms were recorded in a solution containing 5.0 mM [Fe(CN)₆]³⁻,

FIGURE 3 (A) Percent transmittance change at 515 and 755 nm with respect to time and (B) kinetic parameters obtained for thienopyrrole based conjugated polymer (PFTBDT) thin film in 0.1 M TBAPF₆/ACN solution at 515 and 755 nm [Color figure can be viewed at wileyonlinelibrary.com]

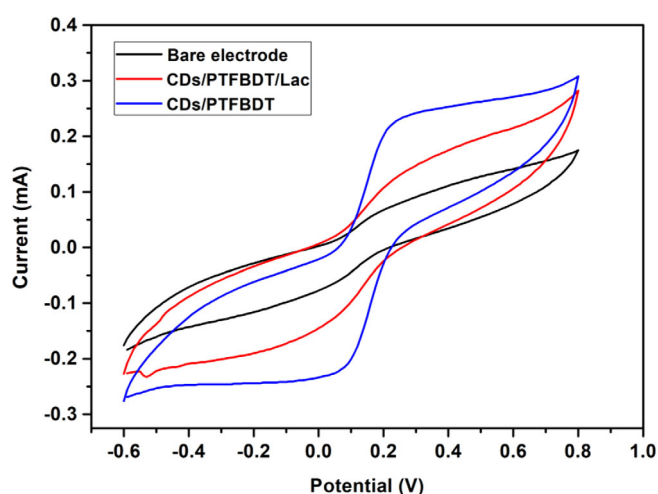
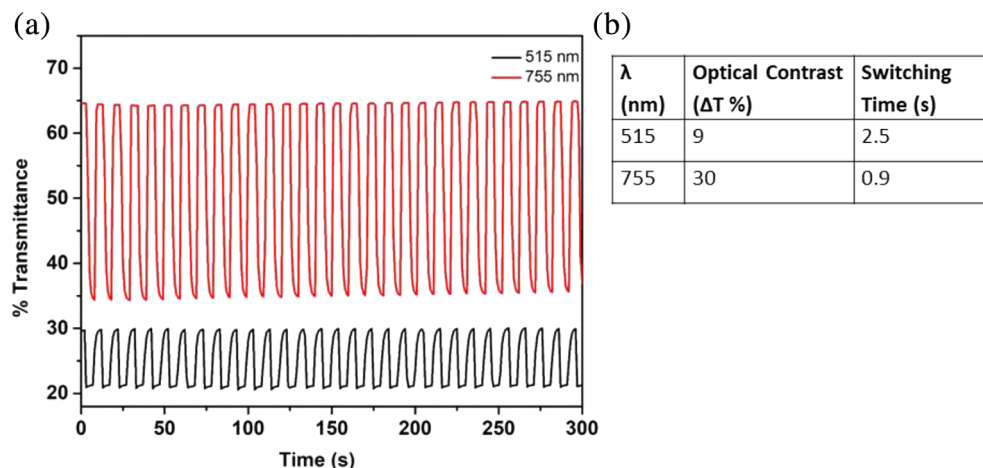
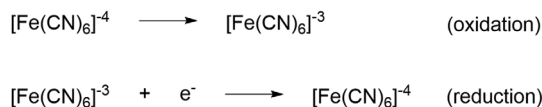


FIGURE 4 Cyclic voltammograms of GE, modified GE/CDs/PFTBDT, and GE/CDs/PFTBDT/Lac electrodes. CDs, carbon dots; GE, bare graphite electrode; Lac, laccase; PFTBDT, thienopyrrole based conjugated polymer [Color figure can be viewed at wileyonlinelibrary.com]

[Fe(CN)₆]⁴⁻, 50 mM phosphate buffer solution (pH 7.0) and 0.1 M KCl under a potential range between -0.6 and 0.8 V at 100 mV/s scan rate. Figure 4 displays the CVs of the bare graphite electrode (GE), modified electrode (GE/CDs/PFTBDT) and modified electrode with laccase enzyme (GE/CDs/PFTBDT/Lac) at ambient temperature. Randles-Sevcik equation affirms the direct relation between effective surface area and the peak current.³⁹ The reaction taking place on the working electrode is as the following;



Here, at bare GE electrode, the peak current was obtained as 86 μA . The peak current jumped to the value of 202 μA in the GE/CDs/PFTBDT electrode. The enhancement in the peak current proves the effect of charge transfer on effective surface area of the modified GE/CDs/PFTBDT electrode (0.21 cm²). When laccase enzyme was immobilized onto modified GE/CDs/PFTBDT electrode, peak current was recorded as 150 μA . The decrease in the peak current resulted from the insulating character of the biomolecule indicates the effective immobilization of the enzyme molecule onto the modified electrode.

Figure 5 displays the surface characterizations of GE/CDs/PFTBDT and GE/CDs/PFTBDT/Lac electrodes by SEM. Surface morphology of the only carbon dot-coated graphite electrode was not observable with SEM. That is attributed due to small size of the CDs. Image of GE/CDs/PFTBDT film shows the uniform cauliflower structure (Figure 5(A)). This uniform cauliflower structure increased the effective surface area and provided a proper surface for enzyme immobilization. After laccase immobilization, surface of the electrode became smoother compared to GE/CDs/PFTBDT modified electrode (Figure 5(B)). The smoothness of the surface can be considered as an evidence for successful enzyme immobilization.

3.3 | Optimization of the modified biosensor

First, the parameters such as the amount of carbon dots, PFTBDT, enzyme and pH of the working medium that affect biosensor performance were optimized to enhance the response and performance of the modified biosensor. To determine the optimum amount of CDs, GE/CDs/PFTBDT/Lac electrodes with varying CD concentrations

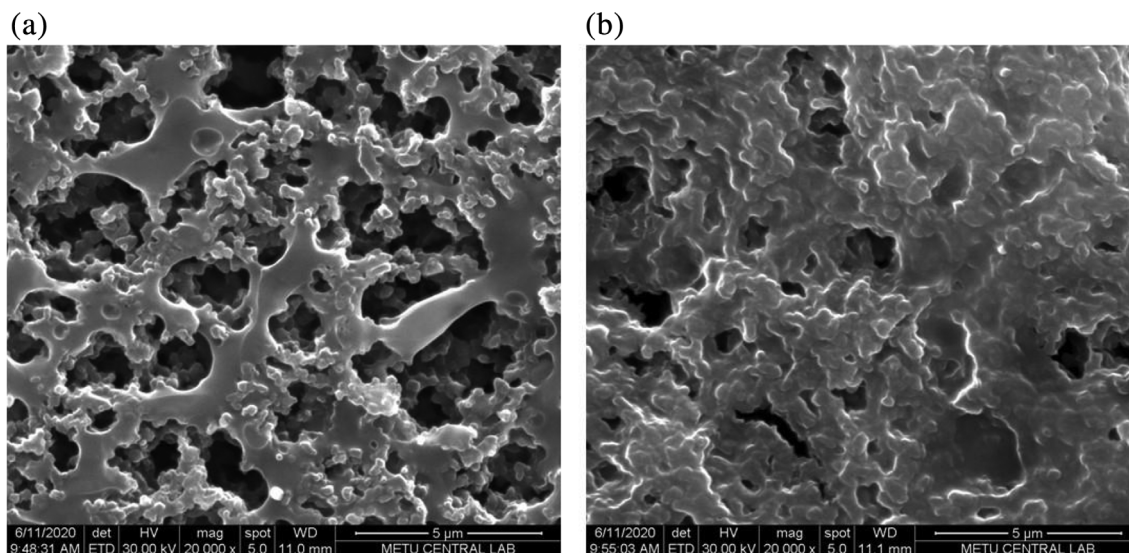


FIGURE 5 SEM images of modified surfaces A) GE/CDs/PFTBDT (B) GE/CDs/PFTBDT/Lac. CDs, carbon dots; GE, bare graphite electrode; Lac, laccase; PFTBDT, thienopyrrole based conjugated polymer

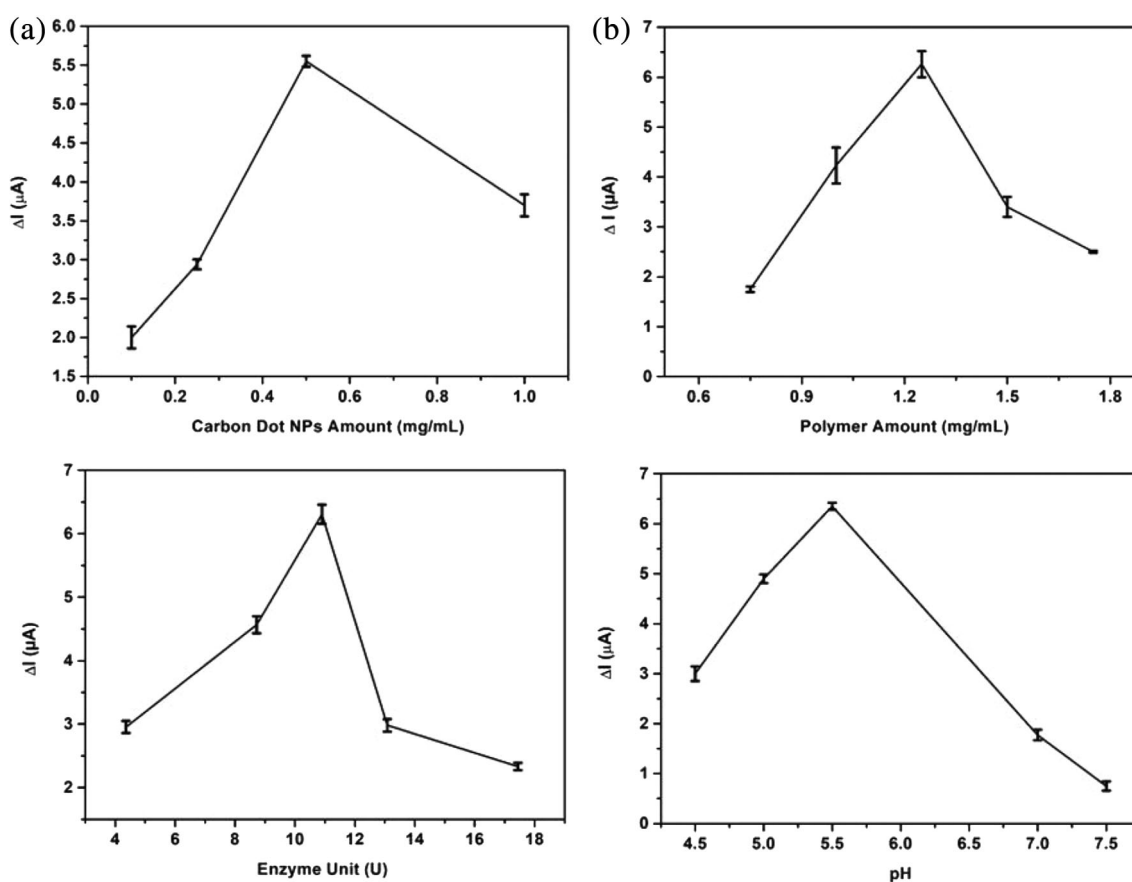


FIGURE 6 The effect of (A) CD amount, (B) polymer amount, (C) laccase amount and (D) pH on laccase biosensor response

ranging between 0.1 and 1.0 $\text{mg}\cdot\text{mL}^{-1}$ were prepared and tested (Figure 6(A)). The best response towards catechol was achieved with 0.5 $\text{mg}\cdot\text{mL}^{-1}$ CD concentration as

depicted in Figure 6(A). Therefore, in the further optimization steps, CD concentration was kept constant at 0.5 $\text{mg}\cdot\text{mL}^{-1}$. The PFTBDT amount was optimized via

using polymer solutions with varying PFTBDT concentration on the CD coated GE electrode (GE/CD). The polymer solutions with PFTBDT concentrations of 1.75, 1.50, 1.25, 1.0 and 0.75 mg.ml⁻¹ were tested to obtain the best response. The highest signal was recorded for the GE/CDs/PFTBDT/Lac electrode with 1.25 mg.ml⁻¹ PFTBDT (Figure 6(B)). Here, the higher concentrations of PFTBDT were found to be preventing the electron transfer, while the lower concentrations of PFTBDT were found to be insufficient for effective charge transfer. The laccase amount was optimized next. To determine the optimum enzyme amount, different amounts of enzyme (4.36–17.44 U) were immobilized onto GE/CDs/PFTBDT. The highest response for catechol biosensing was obtained with 10.9 U of laccase as given in Figure 6(C). For enzyme activity, the pH of the working medium is also extremely important. Accordingly, to determine the best response of the laccase biosensor, the sensor was tested in different buffer solutions with varying pH values (pH 4.5–7.5). For GE/CDs/PFTBDT/Lac biosensor, the highest current was obtained in acetate buffer solution at pH 5.5 (Figure 6(D)). In addition, the optimization experiments for constructed biosensor were performed in the presence of 125 μM catechol at room temperature.

3.4 | Analytical merits of the catechol biosensor

Analytical characterization of the catechol biosensor was examined under the optimized conditions at -0.3 V. The

amperometric response of the modified biosensor was monitored via the injection of varying catechol amounts. For GE/CDs/PFTBDT/Lac biosensor, the LDR was obtained between 1.25 and 175 μM catechol with the equation of $y = 48.31x + 0.4147$ ($R^2 = 0.9994$), while the LOD was calculated as 1.23 μM based on $S/N = 3$ (Figure 7(A)). Amperometric responses of the modified electrode in presence of different concentrations of catechol were also represented in Figure 7(B). Additionally, sensitivity of the biosensor was calculated as 737.4 μA.mM⁻¹.cm⁻² and the response time of the developed biosensor was about 8 s. Stability of the catechol detection using GE/CDs/PFTBDT/Lac biosensor was also verified via the recording of amperometric response for 10 measurements under the optimized conditions in the presence of 125 μM catechol in reaction medium. In order to test the reproducibility, three different electrodes were prepared with the same modification and the response of these three electrodes showed low standard deviation in the presence of 125 μM catechol. The SD of 10 measurements was found to be as ±0.072, and SD of measurements of three different electrodes was found to be as 7.80% indicating the reproducibility, high reliability and the robustness of the developed biosensor.

Analytical performance of the developed catechol biosensor was compared to other catechol biosensors using the same laccase system in Table 1. The comparison clearly reveals the wider LDR, lower LOD and higher sensitivity of the developed biosensor in this work.

Finally, the interference effects on the proposed biosensor was investigated in the presence of different

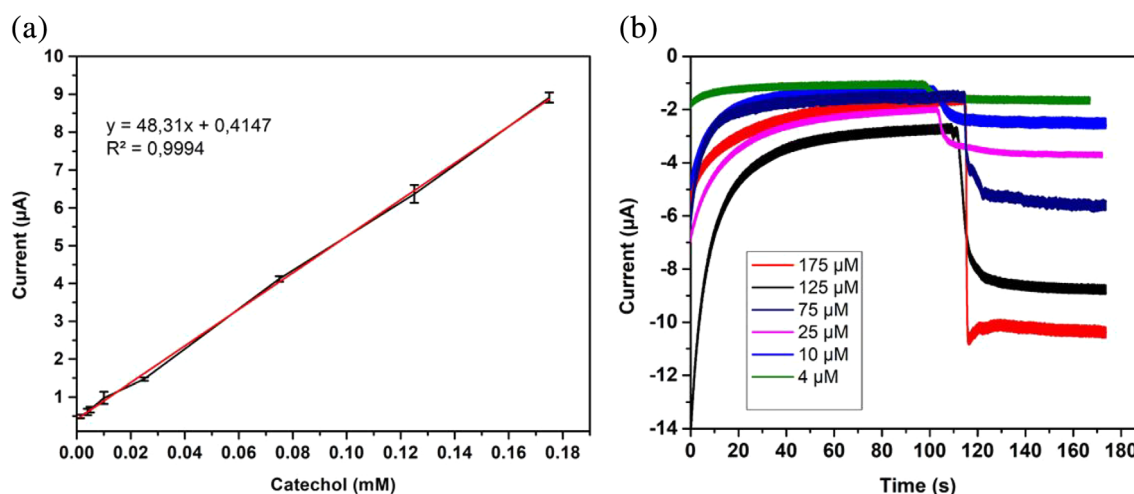


FIGURE 7 (A) Calibration curve of the modified electrode for catechol (in 50 mM acetate buffer, pH 5.5, 25°C, -0.3 V) (B) Amperometric responses of the modified electrode in the presence of different concentrations of catechol [Color figure can be viewed at wileyonlinelibrary.com]

TABLE 1 Analytical merits comparison of the proposed biosensor and the previously reported laccase-based biosensors for electrochemical detection/sensing of catechol

Substrate(s)	Modified electrode	Detection technique	Stability (%) ^a or reproducibility ^b	Sensitivity ($\mu\text{A cm}^{-2}\text{mM}^{-1}$)	LOD (μM ; single CAT)	LDR (μM)	Sample(s) for method application	References
Catechol	AgNPs-Pdop@Gr/GCE	DPV	2.0 ^b	NR	0.1	0.5–240	Pond water	40
Catechol and hydroquinone	P4VPBA/PPy/GO/GCE	CV/DPV	6.34 ^b	NR	0.96	7.0–16	Tap water	41
Catechol and hydroquinone	AuNPs/ZnO/Al ₂ O ₃ /GO, chit/GCE	CV	93.1 ^a	NR	3.10	0.5–40	Local water sample	42
Catechol	GO/PM/GCE	DPV	90.1 ^a	537.0	0.008	0.03–138	Ground and tap water	43
Catechol	Lac-F, N-CDS/GCE	CV, <i>i-t</i>	11.76 ^b	219.17	0.014	12–450	Tap and lake water	44
Catechol	Lac-a-Fe ₂ O ₃ NC-CPE	<i>i-t</i>	4.0 ^b	NR	4.28	8–800	Tap water and Textile industry effluent	45
Catechol and hydroquinone	PCH/AGCE	DPV	3.03 ^b	NR	0.066	1–300	Tap and lake water	46
Catechol	MOF-ERGO-5/GCE	DPV	97.0	NR	0.1	0.1–566	Tap water	47
Catechol	CPE-B	CV	3.6 ^b	232.0	~1	~12.7–142.6	Green tea sample	48
Catechol	SPEs/MWCNTs/AuNWs/Tyr	<i>i-t</i>	NR	NR	0.027	0.5–42	—	49
Catechol and hydroquinone	rGO-Fe ₃ O ₄ -au/GCE	DPV	2.3 ^b	NR	0.02	0.05–550	Artificial wastewater	50
Catechol, hydroquinone bisphenol A and phenol	AgNPs/MWCNT/GCE	SWV	2.6 ^b	~310	0.2	20–260	Tap water	51
Catechol and hydroquinone	CS/MWCNTs/PDA/AuNPs/GCE	DPV	1.38 ^b	NR	0.047	0.1–10	Tap and lake water	52
Catechol and hydroquinone	Lac/AP-rGOs/chit/GC	<i>i-t</i>	3.96 ^b	15.79	7.0	15–700	Tap and lake water	53
Catechol	Lac/PFTBTD/CDs/GE	<i>i-t</i>	1.10 ^b	737.44	1.2	1.25–175	Tap water	This work

Abbreviations: AuNWs, gold nanowires; CD, carbon dots; CPE, carbon paste electrode modified with banana tissue; CV, cyclic voltammetry; DPV, differential pulse voltammetry; GCE, glassy carbon electrode; LDR, linear dynamic range; LOD, limit of detection; MOF, metal-organic framework; MWCNTs, multi-walled carbon nanotubes; NR, not reported; P4VPBA, poly (4-vinylphenylboronic acid); rGO, reduced graphene oxide; SWV, square wave voltammetry.

^aStability

^bReproducibility.

substrates. Urea, ethanol and ascorbic acid were used as the interfering agents. A volume of 0.05 mM of these agents were injected into 50 mM acetate buffer at pH 5.5. Results showed that there was no obvious current change in the presence of interfering agents. On the other hand, response of the modified electrode was highly stable towards catechol (Figure 8(a)). The results obtained in here clearly demonstrates the specificity and the sensitivity of the proposed biosensor for catechol detection. Apart from interfering substances, response of the electrode to other phenolic compounds was investigated. A volume of 0.05 M of catechol, phenol and hydroquinone were injected to the system and the only non-negligible response obtained was belonging to the catechol (Figure 8 (B)). This clarifies that the proposed system was highly specific to catechol.

3.5 | Real sample analysis

The analytical applicability of the proposed biosensor was investigated using tap water. Results are given in Table 2. Recoveries were obtained by determination of catechol concentration in the tap water sample after spiking with known concentrations of catechol. Three different concentrations (125 μ M, high 25 μ M, medium and 5 μ M, low) of catechol was chosen for the spiking experiments. The quantitative recoveries were found to be as 104, 100 and 96% for the spiked catechol concentration of 125, 25, and 5 μ M, respectively. The recoveries which are near 100% clearly indicates the reliability of the method for catechol detection. The obtained data proved that the GE/CDs/PFTBDT/Lac biosensor was highly accurate and effective for the detection of catechol in real samples.

3.6 | Computational results

Two different conformations were determined for PFTBDT tetramer. Thiophene sulfur of the TPD acceptor and furan bridge oxygen have the same direction in the first conformer (Figure 9(A)). This conformer (conf1) has a star shape from the edge view due to the dihedral angle 6° angle between TPD and furan at the both sides and 10° average angle between donor group and furan bridge. Furan oxygens and pyrrole-4,6(5H)-dione oxygens are on the same side in the second structure (conf2) where dihedral angle between TPD and furan group as well as donor and furan group are less than 2° in the optimized geometry as given in Figure 9(B). Although conf2 has highly planar geometry which makes it a better candidate as donor-acceptor conducting copolymer, star shaped conf1 of PFTBDT tetramer is 0.31 eV more stable per donor-acceptor pair due to the repulsion between furan oxygens and pyrrole-4,6(5H)-dione oxygens in conf2. DFT calculations performed for both conformers since molecular mechanics calculations (Supporting Information) showed that planar conf2 is more stable in multichain packing structure contrary to the single chain energy comparison. This means that both low density star shaped conf1 and planar well-packed conf2 can present in the PFTBDT film. ESP mapped onto the conf1 and conf2 showed that both polymers show a sequential well-differentiated

TABLE 2 Determination of catechol in tap water

Sample	C_{added} (mM)	C_{found} (mM)	Recovery (%)
Tap water	0.125	0.130	104
	0.025	0.025	100
	0.005	0.0048	96

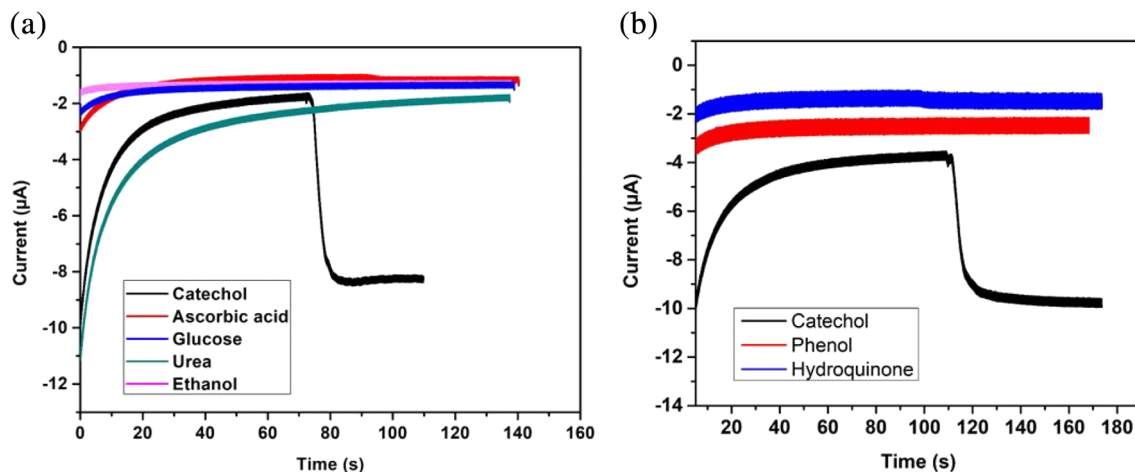


FIGURE 8 The response of the modified biosensor toward (A) different substrates including catechol (B) phenol derivatives including 125 μ M catechol in 50 mM acetate buffer (pH 5.5) at -0.3 V [Color figure can be viewed at wileyonlinelibrary.com]

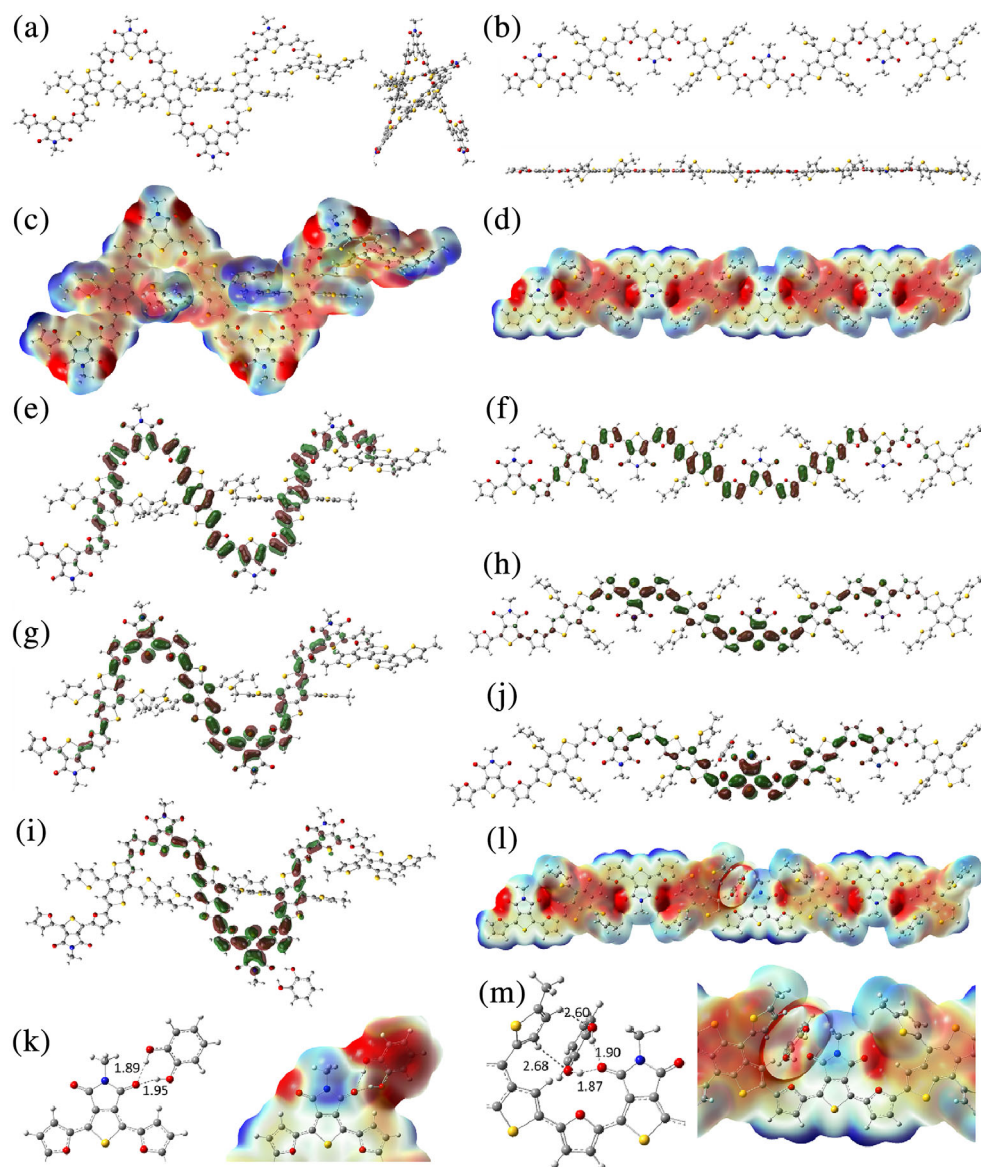


FIGURE 9 (A) Star shape conformation of thienopyrrole based conjugated polymer (PFTBDT) (conf1), (B) planar conformation of PFTBDT (conf2), (C) Electrostatic potential surface (ESP) of conf1, (D) ESP of conf2, (E) Contour plots of the highest occupied molecular orbitals (HOMO) for conf1, (F) HOMO for conf2, (G) lowest unoccupied molecular orbitals (LUMO) for conf1, (H) LUMO for conf2, (I) LUMO for conf1 and catechol complex, (J) LUMO for conf2 and catechol complex, (K) interaction and ESP of conf1 and catechol complex, (L) ESP of conf2 and catechol complex, (M) interaction and ESP of conf2 and catechol complex [Color figure can be viewed at wileyonlinelibrary.com]

donor-acceptor structures (Figure 9(C),(D)). Highest electron density was interestingly observed on the pyrrole-4,6 (5H)-dione oxygens of TPD acceptor that overlap with the high electrostatic potential of electron donor groups. This was valid for both conformers, especially can clearly be seen in the ESP of conf2 (Figure 9(D)). Overlap of electron density of TPD oxygens with donor is one of the important properties that provide enhanced effective coupling between the electron donor and acceptor groups and put TPD forward as an acceptor when it is used with suitable donor.⁵⁴

Both HOMO and LUMO orbitals mapped on the PFTBDT are delocalized and distributed along the chain (Figure 9(E)-(H)). Optical band gap was determined as 1.93 and 1.75 eV for conf1 by B3LYP and TPSSH functionals, respectively. There wasn't a significant difference between band gap values of conf1 and conf2. Hole reorganization energies are as low as 0.07 eV and 0.08 eV for

two conformers which indicates high carrier mobilities for the pristine state.

Catechol formed two hydrogen bonding interactions with the pyrrole-4,6(5H)-dione oxygen on TPD acceptor in the lowest energy complex formed by PFTBDT and catechol. Although HOMO orbital does not show any significant difference, LUMO orbitals are more localized onto the TPD acceptor which form complex with catechol (Figure 9(I),(J)). ESP maps point out a significant charge transfer from PFTBDT to catechol and disruption in the sequential (Figure 9(L),(M)). The amount of charge transfer from polymer to catechol based on the electrostatic potential fitting⁵⁵ is determined as 0.04 e⁻/catechol for both conformers. Vertical electron affinity became more negative from -2.2 eV to -2.4 eV and vertical ionization energy is increased from 5.6 eV to 5.7 eV for pristine and catechol interacted PFTBDT. Most importantly, basis set

superposition error corrected interaction energy between catechol and PFTBDT is calculated as -0.46 and -0.57 eV per catechol for conf1 and conf2, respectively. Higher interaction energy observed for planar conf2 is due the additional interaction between donor side chain hydrogens and oxygen atoms of catechol (Figure 9(M)). Two strong hydrogen bonds between catechol and PFTBDT, charge transfer from polymer to catechol, disruption of electrostatic potential surface, localization of unoccupied orbitals on the acceptor group were determined as the main mechanisms for the observed current decrease given in Figure 8 leading to the successful design of catechol electrochemical biosensor with high sensitivity and selectivity by using PFTBDT.



4 | CONCLUSIONS





In this study, the construction of a catechol electrochemical biosensor by laccase immobilization onto the modified working electrode via physical adsorption technique was reported. Modification was provided with CDs and PFTBDT coating on the graphite electrode. The proposed enzyme-based biosensor was optimized in terms of amount of carbon dots, amount of PFTBDT, enzyme unit and pH. The constructed biosensor exhibited linearity between 1.25 and 175 μM catechol, with a LOD of 1.23 μM and sensitivity of 737.4 $\mu\text{A}\cdot\text{mM}^{-1}\cdot\text{cm}^{-2}$. The probe was also highly selective toward catechol such that it did not show any response to the tested interfering agents. The applicability of the biosensor was demonstrated in tap water via the obtained high recovery rates. In conclusion, a novel, robust and a highly sensitive biosensor for catechol determination using carbon dots and PFTBDT was developed in here and compared to the previously reported studies the developed biosensor is advantageous due to its wider LDR, lower LOD and higher sensitivity. We believe the developed method can be a reliable alternative to the routine quantification of catechol in various matrices.

ACKNOWLEDGMENTS

Erol Yildirim gratefully acknowledge support from 2232 International Fellowship for Outstanding Researchers Program of TÜBİTAK (Project No: 118C251). We would like to thank Zeynep İrem Bulut for the synthesis of carbon dots and Prof. Aysen Yilmaz and her group members for providing the opportunity for CD synthesis.

ORCID

Mustafa Yasa  <https://orcid.org/0000-0002-2531-4482>
 Mehrdad Forough  <https://orcid.org/0000-0001-5475-1203>

Erol Yildirim  <https://orcid.org/0000-0002-9989-9882>
 Ozgul Persil Cetinkol  <https://orcid.org/0000-0002-6632-6981>
 Yasemin Arslan Udum  <https://orcid.org/0000-0003-0711-2139>
 Levent Toppare  <https://orcid.org/0000-0002-0198-4617>

REFERENCES

- [1] W. Liu, L. Wu, X. Zhang, J. Chen, *Anal. Methods* **2014**, *6*, 718.
- [2] A. M. De Luis, J. I. Lombrana, A. Menéndez, J. Sanz, *Ind. Eng. Chem. Res.* **2011**, *50*(4), 1928.
- [3] Q. Ye, F. Yan, D. Kong, J. Zhang, X. Zhou, J. Xu, L. Chen, *Sens. Actuators B* **2017**, *250*, 712.
- [4] T. Kanamori, M. Isokawa, T. Funatsu, M. Tsunoda, *J. Chromatogr., B* **2015**, *985*, 142.
- [5] P. Nagaraja, R. A. Vasanth, K. R. Sunitha, *Talanta* **2001**, *55* (6), 1039.
- [6] Z. Zhao, H. Jiang, in *Biosensors*, Vol. 1, Chapter 1 (Ed: P. A. Serra), Intech, Vukovar **2010**, p. 1.
- [7] A. K. Sarma, P. Vatsyayan, P. Goswami, S. D. Minter, *Biosens. Bioelectron.* **2009**, *24*(8), 2313.
- [8] B. Haghghi, L. Gorton, T. Ruzgas, L. Jönsson, *Anal. Chim. Acta* **2003**, *487*(1), 3.
- [9] J. Yang, W. Li, T. B. Ng, X. Deng, X. Ye, *Front. Microbiol.* **2018**, *8*, 832.
- [10] A. Ramanavicius, Y. Oztekin, Z. Balevicius, A. Kausaite-Mikstiniene, V. Krikstolaityte, I. Baleviciute, V. Ratautaite, A. Ramanaviciene, *Proc. Eng.* **2012**, *47*, 825.
- [11] S. Soylemez, S. A. Bekmezci, S. Goker, L. Toppare, *J. Polym. Sci. Polym. Chem.* **2019**, *57*(23), 2019.
- [12] U. Bulut, S. C. S Sanli, A. Cevher, S. Cirpan, S. Donmez, S. Timur, *J. Appl. Polym. Sci.* **2020**, *137*(43), 49332.
- [13] M. Gerard, A. Chaubey, B. D. Malhotra, *Biosens. Bioelectron.* **2002**, *17*(5), 345.
- [14] Y. Zhang, J. Zou, H.-L. Yip, Y. Sun, J. A. Davies, K.-S. Chen, O. Acton, K.-Y. Jen, *J. Mater. Chem.* **2011**, *21*, 3895.
- [15] H. Ham, H.-S. Kim, D.-H. Hwang, I.-N. Kang, *J. Polym. Sci.* **2020**, *1*, 2755. <https://doi.org/10.1002/pol.20200480>.
- [16] E. W. Muller, A. A. Burney-Allen, J. Shaw, D. L. Wheeler, V. Duzhko, M. Jeffries-EL, *J. Polym. Sci.* **2020**, *58*, 1299.
- [17] X. Guo, H. Xin, F. S. Kim, A. D. T. Liyanage, S. A. Jenekhe, M. D. Watson, *Macromolecules* **2011**, *44*, 269.
- [18] Y. Zou, A. Najari, P. Berrouard, S. Beaupre, B. R. Aich, Y. Tao, M. Leclerc, *J. Am. Chem. Soc.* **2010**, *132*(15), 5330.
- [19] M.-C. Yuan, M.-Y. Chiu, S.-P. Liu, C.-M. Chen, K.-H. Wei, *Macromolecules* **2010**, *43*(17), 6936.
- [20] Y. Zhang, S. K. Hau, H.-L. Yip, Y. Sun, O. Acton, A. K.-Y. Jen, *Chem. Mater.* **2010**, *22*(9), 2696.
- [21] Y.-R. Hong, H.-K. Wong, L. C. H. Moh, H.-S. Tan, Z.-K. Chen, *Chem. Commun.* **2011**, *47*, 4920.
- [22] S. Kurbanoğlu, L. Toppare, *Rev. Roum. Chim.* **2015**, *60*(5), 453.
- [23] Q. Huang, S. Hu, H. Zhang, J. Chen, Y. He, F. Li, W. Weng, J. Ni, X. Bao, Y. Lin, *Analyst* **2013**, *138*(18), 5417.
- [24] S. Bhattacharya, R. Sarkar, B. Chakraborty, A. Porgador, R. Jelinek, *ACS Sens.* **2017**, *2*, 1215.
- [25] M. Li, T. Chen, J. J. Gooding, J. Liu, *ACS Sens.* **2019**, *4*, 1732.
- [26] S. Pandit, T. Banerjee, I. Srivastava, S. Nie, D. Pan, *ACS Sens.* **2019**, *4*, 2730.

- [27] S. Campuzano, P. Yáñez-Sedeño, J. M. Pingarrón, *Nanomaterials* **2019**, 9(4), 1.
- [28] S. Zhu, Q. Meng, L. Wang, J. Zhang, Y. Song, H. Jin, K. Zhang, H. Sun, H. Wang, B. Yang, *Angew. Chem., Int. Ed.* **2013**, 52, 4045.
- [29] A. Robitaille, A. Perea, D. Be'langer, M. Leclerc, *J. Mater. Chem.* **2017**, 5, 18088.
- [30] P. J. Stephens, F. J. Devlin, C. F. Chabalowski, M. J. Frisch, *J. Phys. Chem.* **1994**, 98(45), 11623.
- [31] A. D. Becke, *J. Chem. Phys.* **1993**, 98, 5648.
- [32] C. Lee, W. Yang, R. G. Parr, *Phys. Rev. B* **1988**, 37, 785.
- [33] M. J. Frisch, G. W. Trucks, H. B. Schlegel, G. E. Scuseria, M. A. Robb, J. R. Cheeseman, G. Scalmani, V. Barone, G. A. Petersson, H. Nakatsuji, X. Li, M. Caricato, A. Marenich, J. Bloino, B. G. Janesko, R. Gomperts, B. Mennucci, H. P. Hratchian, J. V. Ortiz, A. F. Izmaylov, J. L. Sonnenberg, D. Williams-Young, F. Ding, F. Lipparini, F. Egidi, J. Goings, B. Peng, A. Petrone, T. Henderson, D. Ranasinghe, V. G. Zakrzewski, J. Gao, N. Rega, G. Zheng, W. Liang, M. Hada, M. Ehara, K. Toyota, R. Fukuda, J. Hasegawa, M. Ishida, T. Nakajima, Y. Honda, O. Kitao, H. Nakai, T. Vreven, K. Throssell Jr., J. A. Montgomery, J. E. Peralta, F. Ogliaro, M. Bearpark, J. J. Heyd, E. Brothers, K. N. Kudin, V. N. Staroverov, T. Keith, R. Kobayashi, J. Normand, K. Raghavachari, A. Rendell, J. C. Burant, S. S. Iyengar, J. Tomasi, M. Cossi, J. M. Millam, M. Klene, C. Adamo, R. Cammi, J. W. Ochterski, R. L. Martin, K. Morokuma, O. Farkas, J. B. Foresman, D. J. Fox, *Gaussian 09*, Gaussian, Inc., Wallingford CT **2009**.
- [34] H. T. Turan, O. Kucur, B. Kahraman, S. Salman, V. Aviyente, *Phys. Chem. Chem. Phys.* **2018**, 20, 3581.
- [35] E. A. Alkan, S. Göker, H. Sarigul, E. Yildirim, Y. A. Udum, L. Toppare, *J. Polym. Sci.* **2020**, 58, 956.
- [36] J. P. Perdew, J. Tao, V. N. Staroverov, G. E. Scuseria, *Chem. Phys.* **2004**, 120, 6898.
- [37] J. L. Bredas, D. Beljonne, V. Coropceanu, J. Cornil, *J. Chem. Rev.* **2004**, 104(11), 4971.
- [38] H. Sun, S. J. Mumby, J. R. Maple, A. T. Hagler, *J. Am. Chem. Soc.* **1994**, 116, 2978.
- [39] P. Zhu, Y. Zhao, *Mater. Chem. Phys.* **2019**, 233, 60.
- [40] K.-J. Huang, L. Wang, J. Li, M. Yu, Y.-M. Liu, *Microchim. Acta* **2013**, 180, 751.
- [41] H. Mao, M. Liu, Z. Cao, C. Ji, Y. Sun, D. Liu, S. Wu, Y. Zhang, X.-M. Song, *Appl. Surf. Sci.* **2017**, 420, 594.
- [42] M. Nazari, S. Kashanian, P. Moradipour, N. Maleki, *J. Electroanal. Chem.* **2018**, 812, 122.
- [43] S. Palanisamy, S. K. Ramaraj, S.-M. Chen, V. Velusamy, T. C. K. Yang, T.-W. Chen, *Microchim. Acta* **2017**, 184, 1051.
- [44] L. Liu, S. Anwar, H. Ding, M. Xu, Q. Yin, Y. Xiao, X. Yang, M. Yan, H. Bi, *J. Electroanal. Chem.* **2019**, 840, 84.
- [45] C. Sarika, M. S. Shivakumar, C. Shivakumara, G. Krishnamurthy, B. Narasimha Murthy, I. C. Lekshmi, *Artif. Cells. Nanomed. Biotechnol.* **2017**, 45, 625.
- [46] M. Zhang, C.-y. Ge, Y. Jin, L. Hu, H. Mo, X. Li, H. Zhang, *J. Chem.* **2019**, 2019, 1.
- [47] Q. Chen, X. Li, X. Min, D. Cheng, J. Zhou, Y. Li, Z. Xie, P. Liu, W. Cai, C. Zhang, *J. Electroanal. Chem.* **2017**, 789, 114.
- [48] N. Broli, L. Vallja, A. Shehu, M. Vasjari, *J. Food Process. Preserv.* **2019**, 43(6), 1.
- [49] S. Kurbanoglu, S. A. Ozkan, *Electrocatalysis* **2018**, 9, 252.
- [50] T. Shimomura, T. Itoh, T. Sumiya, T.-a. Hanaoka, F. Mizukami, M. Ono, *Sens. Actuators B* **2011**, 153(2), 361.
- [51] L. A. Goulart, R. Gonçalves, A. A. Correa, E. C. Pereira, L. H. Mascaro, *Microchim. Acta* **2018**, 185(12), 1.
- [52] I. C. Lekshmi, I. Rudra, R. Pillai, C. Sarika, M. S. Shivakumar, C. Shivakumara, S. B. Konwar, B. Narasimhamurthy, *J. Electroanal. Chem.* **2020**, 867, 114190.
- [53] X.-H. Zhou, L.-H. Liu, X. Bai, C.-H. Shi, *Sens. Actuators,-B* **2013**, 181, 661.
- [54] T. Kim, J.-H. Kim, T. E. Kang, C. Lee, H. Kang, M. Shin, C. Wang, B. Ma, U. Jeong, T.-S. Kim, B. J. Kim, *Nat. Commun.* **2015**, 6, 8547.
- [55] C. M. Breneman, K. B. Wiberg, *J. Comput. Chem.* **1990**, 11(3), 361.

SUPPORTING INFORMATION

Additional supporting information may be found online in the Supporting Information section at the end of this article.

How to cite this article: Yasa M, Deniz A, Forough M, et al. Construction of amperometric biosensor modified with conducting polymer/ carbon dots for the analysis of catechol. *J Polym Sci.* 2020;58:3336–3348. <https://doi.org/10.1002/pol.20200647>